Acta Pharmacologica Sinica

www.nature.com/aps

ARTICLE

Novel Caspase-1 inhibitor CZL80 improves neurological function in mice after progressive ischemic stroke within a long therapeutic time-window

Ling Pan[1], Wei-dong Tang[1], Ke Wang[1], Qi-feng Fang[1], Meng-ru Liu[1], Zhan-xun Wu[1], Yi Wang[1,2], Sun-liang Cui[3], Gang Hu[4], Ting-jun Hou[3], Wei-wei Hu[1], Zhong Chen[1,2] and Xiang-nan Zhang[1]

Progressive ischemic stroke (PIS) is featured by progressive neurological dysfunction after ischemia. Ischemia-evoked neuroinflammation is implicated in the progressive brain injury after cerebral ischemia, while Caspase-1, an active component of inflammasome, exaggerates ischemic brain injury. Current Caspase-1 inhibitors are inadequate in safety and druggability. Here, we investigated the efficacy of CZL80, a novel Caspase-1 inhibitor, in mice with PIS. Mice and *Caspase-1*$^{-/-}$ mice were subjected to photothrombotic (PT)-induced cerebral ischemia. CZL80 (10, 30 mg·kg^{-1}·d^{-1}, i.p.) was administered for one week after PT onset. The transient and the progressive neurological dysfunction (as foot faults in the grid-walking task and forelimb symmetry in the cylinder task) was assessed on Day1 and Day4-7, respectively, after PT onset. Treatment with CZL80 (30 mg/kg) during Day1-7 significantly reduced the progressive, but not the transient neurological dysfunction. Furthermore, we showed that CZL80 administered on Day4-7, when the progressive neurological dysfunction occurred, produced significant beneficial effects against PIS, suggesting an extended therapeutic time-window. CZL80 administration could improve the neurological function even as late as Day43 after PT. In *Caspase-1*$^{-/-}$ mice with PIS, the beneficial effects of CZL80 were abolished. We found that Caspase-1 was upregulated during Day4-7 after PT and predominantly located in activated microglia, which was coincided with the progressive neurological deficits, and attenuated by CZL80. We showed that CZL80 administration did not reduce the infarct volume, but significantly suppressed microglia activation in the peri-infarct cortex, suggesting the involvement of microglial inflammasome in the pathology of PIS. Taken together, this study demonstrates that Caspase-1 is required for the progressive neurological dysfunction in PIS. CZL80 is a promising drug to promote the neurological recovery in PIS by inhibiting Caspase-1 within a long therapeutic time-window.

Keywords: progressive ischemic stroke; neuroinflammation; Caspase-1 inhibitor; microglia; neurological dysfunction; therapeutic time-window

Acta Pharmacologica Sinica (2022) 43:2817–2827; https://doi.org/10.1038/s41401-022-00913-7

INTRODUCTION

Ischemic stroke is one of the leading causes of death and disability world-wide [1]. Stroke-induced neurological dysfunction, either transient or in a long term, remains a challenge for stroke therapy and rehabilitation. Beside the immediate neurological function loss after ischemic stroke, approximately 1/4 to 1/3 of patients develop progressive ischemic stroke (PIS) characterized by progressively neurological deficits within a few days after the stroke [2]. Patients with PIS have higher mortality, poorer prognosis, and more severe neurological deficits compared with other non-PIS patients [3]. Alleviating the progression of neurological dysfunction significantly improves the long-term recovery in mice, suggesting the potential significance of intervention in progressive stroke [4, 5]. However, it remains largely unclear how PIS develops.

Neuroinflammation plays a central role in neuronal cell death and neurological dysfunction caused by ischemia [6–8]. Excessive neuroinflammation aggravates neurovascular damage and impedes functional recovery, leading to long-term neurological deficits [9, 10]. In PIS patients, the increase of pro-inflammatory factors in serum is closely related to the deterioration of the penumbra [8, 11–13]. However, the direct association of neuroinflammation with PIS has not been fully established.

Inflammasomes is a multiple-protein complex that senses and activates inflammatory responses [14]. Inflammasomal activation is involved in the progressive brain injury after cerebral ischemia [15, 16]. Caspase-1 serves as the active component of the inflammasome [17, 18]. Compared with other components, Caspase-1 is accepted as a druggable target for inflammasomes.

[1]Institute of Pharmacology and Toxicology, College of Pharmaceutical Sciences, Zhejiang University, Hangzhou 310058, China; [2]Key Laboratory of Neuropharmacology and Translational Medicine of Zhejiang Province, School of Pharmaceutical Sciences, Zhejiang Chinese Medical University, Hangzhou 310053, China; [3]Department of Pharmachemistry, College of Pharmaceutical Sciences, Zhejiang University, Hangzhou 310058, China and [4]Department of Pharmacology, School of Medicine and Life Sciences, Nanjing University of Chinese Medicine, Nanjing 210029, China
Correspondence: Zhong Chen (chenzhong@zju.edu.cn) or Xiang-nan Zhang (xiangnan_zhang@zju.edu.cn)
These authors contributed equally: Ling Pan, Wei-dong Tang

Received: 19 December 2021 Accepted: 16 April 2022
Published online: 2 May 2022

In ischemic brains, Caspase-1 is activated in the subacute and recovery phases after cerebral ischemia [19, 20]. Caspase-1 amplifies neuroinflammation and aggravates the neuronal injury by causing cell pyrosis [19, 21]. Moreover, Caspase-1 is involved in neurological deficit and brain edema [22, 23]. Unfortunately, however, the most widely-accepted Caspase-1 inhibitors including Ac-YVAD-cmk, VX-740 and VX-765, are limited by either poor bioavailability or toxicity [24, 25]. To overcome the shortcomings of the current Caspase-1 inhibitors, we previously designed and identified a new Caspase-1 inhibitor, CZL80, which showed promising therapeutic effects on febrile seizures and refractory epilepsy [26, 27]. In the present study, we aimed to explore whether CZL80 was effective to rescue the progressive neurological dysfunction in a photothrombotic stroke model in mice.

MATERIALS AND METHODS

Animals

Male C57BL/6 mice and Caspase-1 gene knockout (*Caspase-1*$^{-/-}$) mice weighing 23–26 g (9–10 weeks old) were used. The *Caspase-1*$^{-/-}$ mice were provided by Prof Gang Hu (Nanjing University of Chinese Medicine, China). Mice were maintained in cages with a 12-h light/dark cycle (lights on from 8:00 to 20:00) and had access to water and food *ad libitum*. Experiments were conducted between 9:00 and 17:00. All experiments were approved by and conducted in accordance with the ethical guidelines of the Zhejiang University Animal Experimentation Committee and were in complete compliance with the National Institutes of Health Guide for the Care and Use of Laboratory Animals. Efforts were made to reduce any pain and the number of animals required.

Photothrombotic model of cerebral ischemia

To induce focal cerebral ischemia, photothrombosis (PT) of cortical microvessels was performed in mice as described previously [5, 28]. Mice were anesthetized with 2% isoflurane and mounted in a stereotaxic device (RWD, China). The skull was exposed by a scalp disinfection and midline incision. A cold light source (diameter 2 mm; 16,000 lux) was placed 1.5 mm lateral from bregma. Rose Bengal dissolved in saline (Sigma-Aldrich, St. Louis, MO, USA, 330000) was administered intraperitoneally at a dose of 100 mg/kg. After 5 min, the brain was illuminated for 15 min through the skull to initiate photothrombosis. After the irradiation, the wound was sutured and disinfected with iodine. Body temperature was maintained at 37 °C by a heat lamp (FHC, Bowdoinham, ME, USA) until the mice woke. Sham mice were subjected to the same procedure but no Rose Bengal injection.

Drug administration

CZL80 was dissolved in mixed solvent (propylene glycol:ethanol: water = 5:1:4) and further diluted in saline. Animals were given CZL80 (10, 30 mg·kg^{-1}·d^{-1}, i.p.) at the indicated time after PT. Sham mice were injected with the same volume of vehicle. We did not find any vehicle effects in our study.

Grid-walking task

The grid-walking task was carried out as previously described with minor modification [5, 28, 29]. The device is a 32 cm × 20 cm × 50 cm (length × width × height) iron frame with a 12 mm square wire mesh above it. Mouse was placed individually on the wire grid for 3 min while being video-recorded. Foot faults and the total normal steps (number of foot faults + number of non-faults) of the forelimb were counted. The foot fault index was calculated as the number of foot faults/total steps × 100%. A camera was positioned beneath the device to video footage to assess the stepping errors (foot faults). A step was considered a foot fault if the forelimbs passed through the grid hole, or the mouse was resting with the grid at the level of the wrist.

Cylinder task

The cylinder experiment is designed according to the characteristics of the animal's vertical attachment to the wall and upward exploration. To evaluate the degree of dependence of the mice on a certain side of the limb, mice were placed in a Plexiglas cylinder (15 cm in height with a diameter of 10 cm) and video-recorded for 5 min to determine forelimb symmetry in exploratory rearing. The video footage was analyzed by calculating the time (in seconds) that each forelimb or both forelimbs were placed on the cylinder wall. The asymmetry index is as follows: (% ipsilateral use) – (% contralateral use). The video was analyzed by individuals who were blinded to these experiments.

Measurement of cerebral blood flow

After the mice were anesthetized at the indicated time after ischemia, the mouse skulls were fixed in a stereotaxic apparatus (RWD, China). After sterilizing the mouse scalp hair, the scalp was cut along the midseam, and the indicator light source of the laser speckle imaging system (RWD, China) was directed to the bregma. After adjusting the focal plane and related parameters, the cerebral blood perfusion in mice was recorded. The blood flow of each experimental mouse was measured before surgery and recorded as the baseline.

Toluidine blue staining

Mice were anesthetized and perfused on day 15 after ischemia, followed by toluidine blue staining. Brain sections were cut into 25 μm sections on a cryostat (Thermo NX50, Germany). Toluidine blue staining was performed on Day15 after ischemic stroke. The slices were stained with 0.03% toluidine blue solution (Sigma-Aldrich, St Louis, MO, USA, 89640) for 2 min. Then, sections were washed in distilled water, decolorized in 75% ethanol and dehydrated in 95% and 100% ethanol for 3 min in each step. The sections were cleared in xylene for 5 min. The sections were mounted and observed under a light microscope (Olympus VS120, Japan). Toluidine blue staining was traced and quantified by ImageJ.

Isolation of primary microglial cells, oxygen-glucose deprivation/reoxygenation (OGD/R) treatment and drug administration

For culturing primary microglial cells, 1 or 3-d-old neonatal C57BL/6J mice were used. In brief, we separated the mouse cerebral cortices gently and digested the cortices with 0.125% trypsin (Solarbio, Beijing, China, T1300). Then the primary mixed glial cells were seeded onto T75 flasks coated with 0.01% poly-*L*-lysine (Sigma-Aldrich, St Louis, MO, USA, P4707). Cells were cultured in DMEM medium containing 10% fetal bovine serum. We isolated the primary microglial cells from astrocytes and collected microglial cells from the culture after dissection for 11–14 days by shaking at 100 rpm for 2 h on a 37 °C rotary oscillator. For OGD treatment, the culture medium was removed and cells were rinsed by warmed PBS and then incubated with glucose-free DMEM medium (Gibco, Grand Island, NY, USA, 11966-025) at 24 h after the cells were seeded. Then, the microglial cells were put in a sealed chamber (Billups Rothenburg, San Diego State, California, USA, MIC-101) and ventilated with mixed gas (5% CO_2 + 95% N_2) for 7 min at 25 L/min. The chambers were sealed and incubated for 2 h at 37 °C. OGD-reperfusion (O-R) was performed by returning the cells to routine culture environment for 1 h at 37 °C. CZL80 was dissolved in dimethyl sulfoxide and diluted to 5 μmol/L, with a final DMSO concentration of 0.1%, and then incubated to the medium before and during OGD.

Western blotting

Western blot analysis was performed as described previously [30]. Briefly, the core of the cerebral infarction and the cortical tissue within a radius of 1 mm around it are dissected and quickly frozen

[31]. The equivalent area was removed from the cortex of mice in the Sham group. The peri-infarct cortex tissues were homogenized in RIPA buffer (20 mmol/L Tris–HCl, pH 7.5, 150 mmol/L NaCl, 1 mmol/L EDTA, 1% Triton X-100, 0.5% sodium deoxycholate (Sigma-Aldrich, St Louis, MO, USA, 30970), and 2% Protease Inhibitor Cocktail Tablets (Roche, Basel, Switzerland, 04693132001)). An aliquot of 40 μg protein from each sample was separated using SDS-PAGE and transferred to a nitrocellulose membrane, which was then blocked with 5% nonfat milk in PBS (pH 7.4). The primary antibodies were as follows: Caspase-1 (1:500, Santa Cruz Biotechnology, Santa Cruz, CA, USA, sc-398715), GAPDH (1:3000, Abcam, Cambridge, UK, ab9485), GSDMD (1:1000, ABclonal, Wuhan, China, A20197), VEGFR-2 (1:1000, Cell Signaling Technology, Bedford, MA, USA, D5B1), IL-4 (1:500, ABclonal, Wuhan, China, A14660), IL-10 (1:500, ABclonal, Wuhan, China, A12255). Secondary antibodies were as follows: HRP against either rabbit or mouse IgG (1:5000, Cell Signaling Technology, Bedford, MA, USA, 7071 and 7072).

Immunofluorescence and image analysis

Mice were euthanized by inhalation of isoflurane. They were then perfused transcardially with 0.9% NaCl followed by 4% PFA. The brains were sectioned by a cryostat (Thermo NX50, Germany) at 25 μm thickness. For immunofluorescence, the sections were permeabilized with 0.1% Triton X-100 for 30 min and blocked in PBS containing 5% donkey serum for 90 min at room temperature, followed by incubation in primary antibody at 4 °C overnight. After that, the primary antibody was removed by rinsing the sections for 3 times in PBS. The sections were then incubated with secondary antibodies for 2 h at room temperature. After being washed, the sections were mounted on slides and coverslipped and finally examined using a confocal laser-scanning microscope (Leica TCS SP8, Solms, Germany) and Fluorescence microscope (Olympus VS120, Japan). The primary antibodies were used as follows: rabbit anti-NeuN (1:500, Millipore, Bedford, MA, USA, 3387626), rabbit anti-Iba1 (1:400, Wako, Osaka, Japan, 019-19741), mouse anti-Caspase-1 (1:100, Santa Cruz Biotechnology, Santa Cruz, CA, USA, sc-398715), rabbit anti-CD31 (1:100, Abcam, Cambridge, UK, ab28364) and rat anti-CD68 (1:200, Abcam, Cambridge, UK, ab201845). Secondary antibodies used were donkey anti-mouse Alexa-594 (1:400, Abcam, Cambridge, UK, ab150108), donkey anti-rabbit Alexa-488 (1:400, Abcam, Cambridge, UK, ab150073) and donkey anti-rat Alexa-488 (1:400, Abcam, Cambridge, UK, ab150153).

Images were quantified using ImageJ by an experimenter blind to treatment groups. Images were collected from four to six random fields in each slide and the experiments were performed at least three times. The images were transferred to 8-bit format and the number of microglia and neurons were counted after setting scale and threshold. Morphological statistics of microglia were obtained using ImageJ. CellSense was used to draw lines at different distances from the infarct area, each line 200 microns apart.

Statistical analysis

All data were collected and analyzed in a blinded manner. Data are presented as the mean ± SEM. The data were evaluated by a one-way ANOVA (analysis of variance) with Tukey's post hoc tests. Statistical comparisons were performed with GraphPad Prism 8. Probability (*P*) values less than 0.05 were considered statistically significant.

RESULTS

CZL80 rescues motor dysfunction after photothrombotic stroke in mice

We previously identified the CZL80 as a Caspase-1 inhibitor [26, 27] (Fig. 1a). To examine the effect of CZL80 on neurological function after cerebral ischemia, a photothrombosis (PT) model in mice was employed. After PT onset, mice were administered CZL80 intraperitoneally (*i.p.*) daily for 7 days at the dosage of 10 and 30 mg/kg. The mice were tested for foot fault in the grid-walking task and forelimb asymmetry in the cylinder task in the next 14 days after PT (Fig. 1b). The rate of foot fault and forelimb asymmetry increased at Day1 after PT onset, suggesting the motor dysfunction after acute ischemia. Both the measurements recovered at Day2-3 but exacerbated afterwards and reached the peak at Day7. Subsequently, the motor function was partially ameliorated during Day7-9 and lasted at least to Day14 after PT (Fig. 1c, d). The motor dysfunction at Day4-7 after ischemic in mice recapitulates the features of progressive ischemic stroke [2, 3, 32], and was in consistent with previous studies [5, 33].

We assessed the efficacy of CZL80 on motor dysfunction in the PT model. Compared with the PT group, CZL80 treatment during Day1-7 (10, 30 $mg{\cdot}kg^{-1}{\cdot}d^{-1}$, *i.p.*) showed no significant alternation on the motor function during Day1-3. Remarkably, both the rate of foot fault and forelimb asymmetry were significantly reduced during Day4-7 by CZL80, in a dose-dependent manner. The benefits of 30 mg/kg CZL80 on motor function remained during Day8-14, at which time CZL80 was withdrawn (Fig. 1c, d). These results suggested that CZL80 has minimum effect on acute ischemic injury but can protect against the progressive functional loss after cerebral ischemia.

We next determined the Caspase-1 expression in the peri-infarct cortex of mice at indicated time point after PT. Activated Caspase-1 (p20) increased along with ischemia within 7 days after PT and peaked at Day7, whereas interleukin-1β (IL-1β) did not show alternations accordingly (Fig. 1e). The activation of Caspase-1 was temporally coincided with the time-window of progressive functional impairment of mice in the PT model, suggesting the potential involvement of Caspase-1 in the progressive motor dysfunction. In consistent, we verified the inhibitory effect of CZL80 on Caspase-1 in ischemic brains (Fig. 1f). Collectively, we established a PIS model in mice, which was characterized by a progressive motor dysfunction peaked at Day7. Caspase-1 activation was coincided with the progressive neurological deficits, which was attenuated by CZL80.

Delayed administration of CZL80 is competent to attenuate the progressive neurological dysfunction induced by photothrombosis

We found the acute and progressive motor dysfunction peaked at Day1 and Day7 after PT onset, and CZL80 showed efficacy predominantly against the progressive motor dysfunction. These results forced us to ask whether delayed administration of CZL80 covering Day4 to Day7, the period in which progressive motor function deteriorated, will be sufficient to rescue neurological deficits. To this end, CZL80 either 10 or 30 mg/kg was administered daily during Day1-4 or Day4-7 after PT (Fig. 2a). Compared with the PT group, the rate of foot fault and forelimb asymmetry hardly changed with the treatment of CZL80 during Day1-4. (Fig. 2b, c). However, to our surprise, administration of CZL80 during Day4-7 significantly reduced the motor dysfunction within 14 days after PT (Fig. 2d, e). Furthermore, administration of CZL80 during Day4-7 showed comparable effect with that by Day1-7 treatment in improving motor function (Supplementary Fig. S1a, b). Overall, these results supported that CZL80 counteracted the progressive neurological dysfunction caused by focal cerebral ischemia. Noteworthy, the present data indicated a wide therapeutic time-window of CZL80 to treat PIS.

CZL80 attenuates long-term motor dysfunction after photothrombotic stroke

We next determined the efficacy of CZL80 on long-term neurological function after cerebral ischemia. We found that 30 mg/kg, but not 10 mg/kg, CZL80 administration during Day4-7

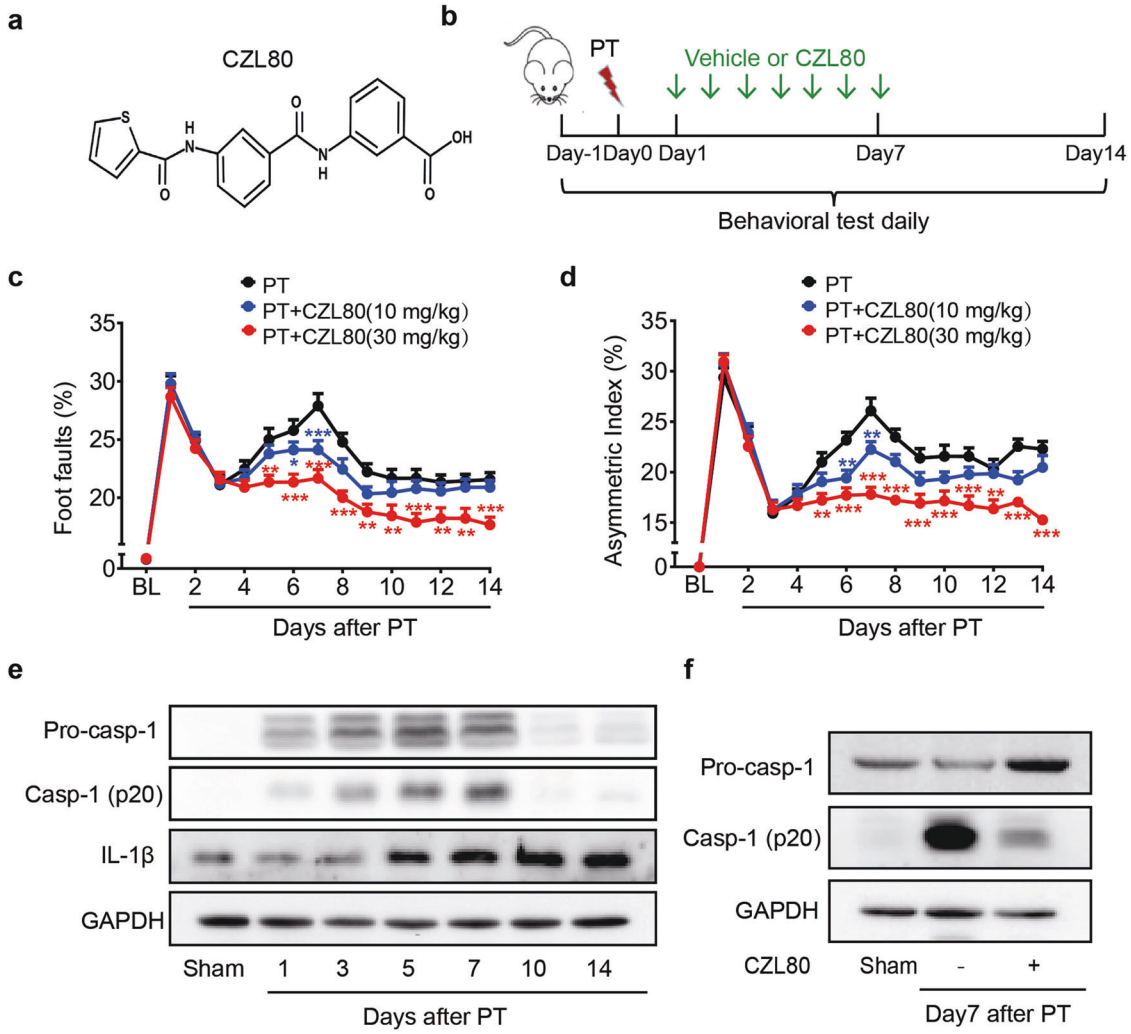

Fig. 1 CZL80 rescues progressive motor dysfunction in photothrombotic mice. a The chemical structure of CZL80. **b** Diagram showing the experimental design in this figure. CZL80 (10 or 30 mg·kg^{-1}·d^{-1}) or vehicle was intraperitoneally injected daily during Day1-7 after photothrombosis (PT), and the motor function was measured daily. **c** Foot fault of left forelimb in the grid-walking task and (**d**) Forelimb asymmetry in the cylinder task. All results were presented as means ± SEM ($n = 9$ per group). Statistical significance was determined by using one-way ANOVA with Tukey's post hoc test, $^{*}P < 0.05$, $^{**}P < 0.01$ and $^{***}P < 0.001$ vs. PT. **e** Representative immunoblots showing the expression of Caspase-1 and IL-1β in the peri-infarct cortex of mice at indicated time points after PT. **f** Representative immunoblots showing the expression level of Caspase-1 with or without CZL80 in the peri-infarct cortex of mice on Day7 after PT.

significantly reduced the rate of foot fault and forelimb asymmetry on Day8, 15, 29, 43 after PT onset ($P < 0.001$ *vs.* PT group, Fig. 3a–c).

Caspase-1 deletion abolishes the therapeutic effect of CZL80

To further investigate whether the effect of CZL80 is attributable to Caspase-1 inhibition, Caspase-1 gene knockout (*Caspase-1*$^{-/-}$) mice were administered 30 mg/kg CZL80 daily during Day4-7 after PT (Fig. 4a). Interestingly, *Caspase-1*$^{-/-}$ mice did not develop progressive neurological dysfunction after PT onset. Moreover, CZL80 failed to show any effect in *Caspase-1*$^{-/-}$ mice (Fig. 4b, c). These results indicated that CZL80 conferred its benefits by inhibiting Caspase-1.

CZL80 cannot ameliorate ischemia-induced neuronal death in progressive stroke

Neuronal cell death plays a critical role in causing neurological deficits after ischemia. In particular, Caspase-1 activation leads to pyroptosis and contributes to ischemic brain injury [19, 34, 35]. We examined whether CZL80 attenuated neuronal cell death after PT. As shown in Fig. 5a, immunofluorescence of NeuN was used to observe the number of neurons in brain cortex at Day1 and Day7 after PT. Compared with the sham group, the number of survived neurons in the peri-infarct cortex was significantly reduced at Day1 but did not further decline along with ischemia. Additionally, CZL80 failed to attenuate the neuronal loss in cortex either at Day1 or at Day7 after PT (Fig. 5a, b). Accordingly, the infarct volume at Day14 was not reduced by continuous treatment with CZL80 for 7 days after PT, as measured by toluidine blue staining (Fig. 5c, d). Caspase-1 cleaves Gasdermin D (GSDMD) to generate GSDMD N-terminus (N-GSDMD), which induces pyroptosis. We found increased N-GSDMD on Day1, which was partly inhibited by CZL80. However, N-GSDMD cannot be reversed by CZL80 on Day7 (Fig. 5e). Overall, these data suggested that reduced neuronal death may not be the predominant mechanism underlying the effect of CZL80 in preventing progressive neurological dysfunction.

CZL80 inhibits microglial activation in PT-induced progressive ischemia

In ischemic brains, Caspase-1 can be activated either in neurons or in microglial cells. We further determined the distribution of

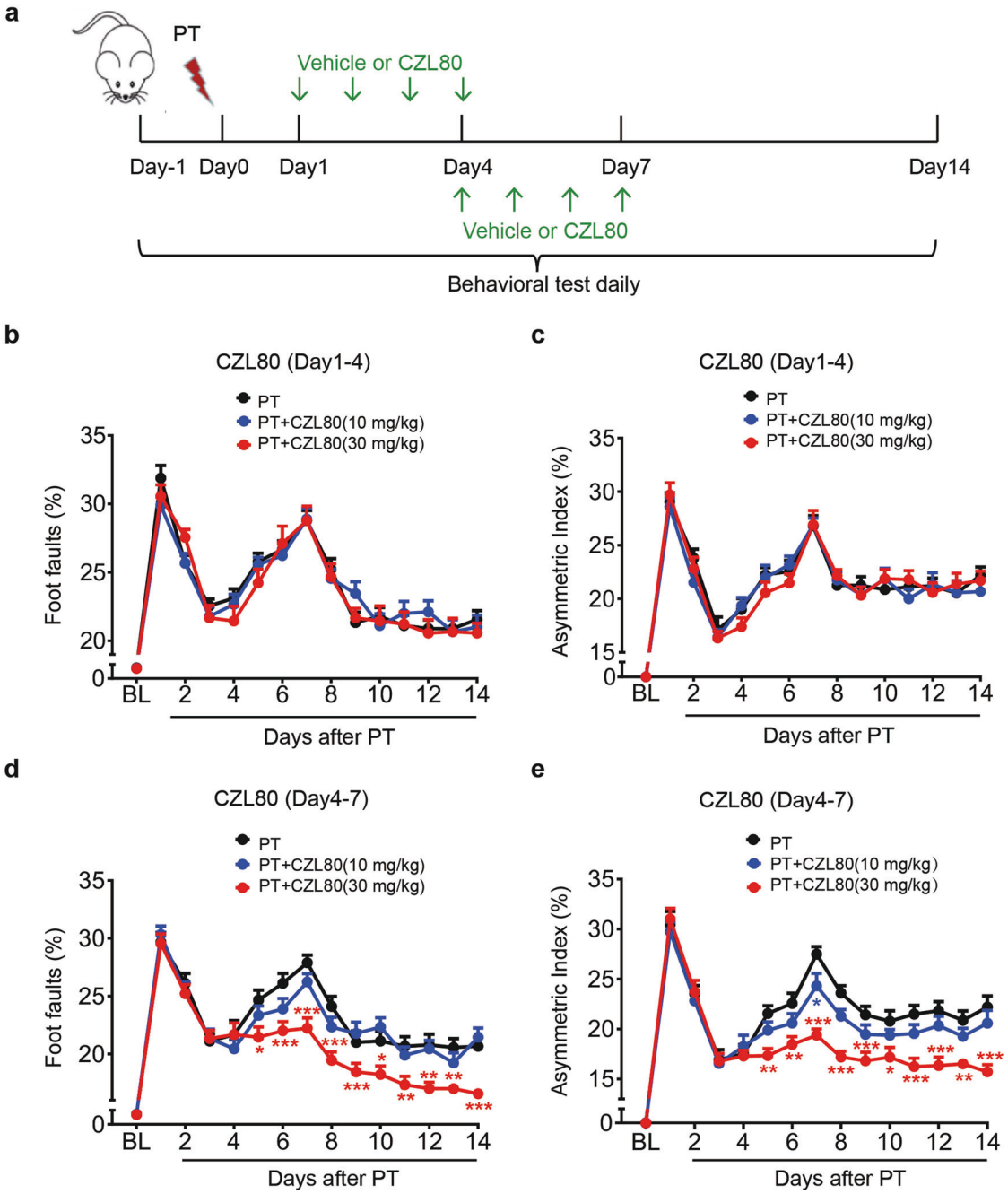

Fig. 2 Treatment with CZL80 during Day4-7, but not Day1-4 after photothrombosis ameliorates progressive neurological dysfunction. **a** Diagram showing the design of the experiments in this figure. CZL80 (10 or 30 mg·kg^{-1}·d^{-1}) or vehicle was intraperitoneally injected daily during Day1-4 or Day4-7, and motor function was measured daily after photothrombosis (PT). **b** Foot fault of left forelimb in the grid-walking task and (**c**) Forelimb asymmetry in the cylinder task with CZL80 administration during Day1-4 after PT. **d** Foot fault of left forelimb in the grid-walking task and (**e**) Forelimb asymmetry in the cylinder task with CZL80 administration during Day4-7 after PT. All results were represented as means ± SEM ($n = 9$ per group). Statistical significance was determined using one-way ANOVA with Tukey's post hoc test, $^{*}P < 0.05$, $^{**}P < 0.01$ and $^{***}P < 0.001$ vs. PT.

Caspase-1 in ischemic brains at Day7 after PT by immunofluorescence staining. Caspase-1 was intensively stained in infarct brain cortex. Moreover, Caspase-1 was colocalized with microglia (Iba-1), but not with neurons (NeuN) or astrocytes (GFAP) in infarct brain tissue (Supplementary Fig. S2). We further quantified the number of microglia surrounding the infarct within 14 days after PT onset. Because the infarcted brain underwent edema or collapsing along with the ischemia, to overcome the errors in counting the microglia, the cortex surrounding the infarct core was divided into 3 areas by their distance (200, 400 and 600 μm) to the edge of core (Fig. 6a). The microglia density in each area was analyzed. The data clearly indicated a progress increase of microglia, which started at Day4 and peaked at Day7, and the increase was most pronounced within 200 μm from the infarct core (Fig. 6b). Moreover, the extension of activation was determined by microglial morphology. The results indicated microglia activation peaked at Day7, as revealed by increased soma area, circularity, and solidity (Fig. 6c–e). The above-mentioned activation of microglia was temporally consistent with the progressive neurological deficit

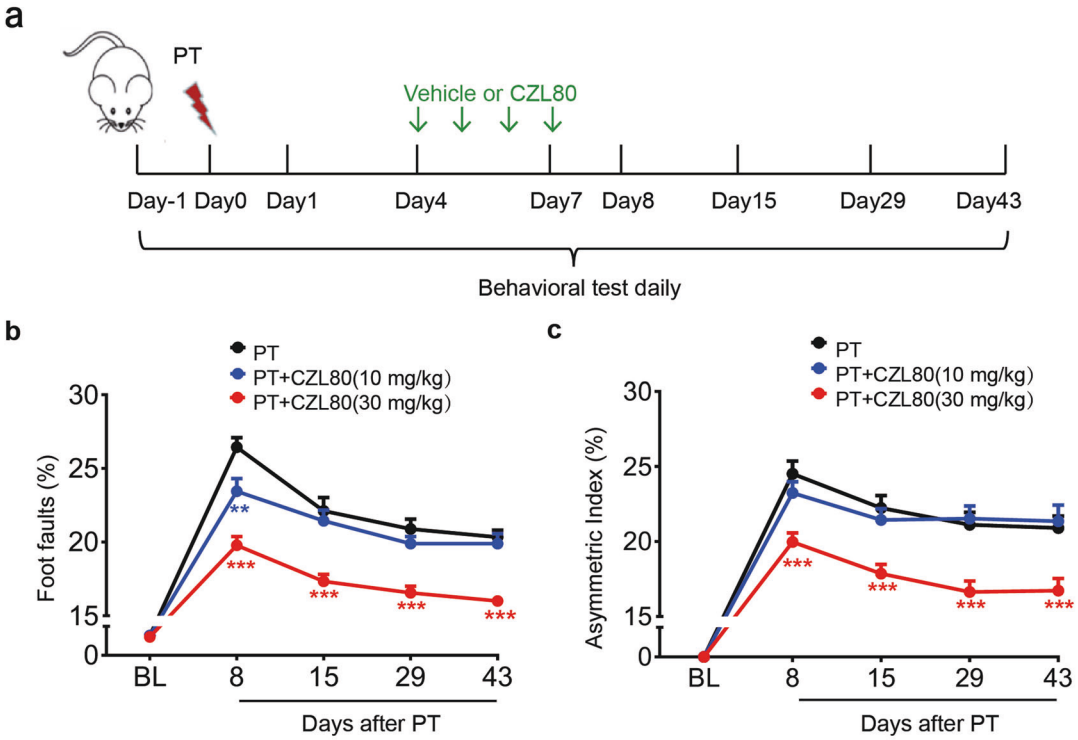

Fig. 3 CZL80 attenuates the long-term motor function recovery after photothrombotic stroke. a Diagram showing the design of the experiments in this figure. CZL80 (10 or 30 mg·kg^{-1}·d^{-1}) or vehicle was intraperitoneally injected daily during Day 4-7 after photothrombosis (PT) and motor function was measured on Day8, 15, 29, 43 after PT. **b** Foot fault of left forelimb in the grid-walking task and (**c**) Forelimb symmetry in the cylinder task were determined. All results were represented as means ± SEM ($n = 9$ per group). Statistical significance was determined using one-way ANOVA with Tukey's post hoc test, $^{**}P < 0.01$ and $^{***}P < 0.001$ vs. PT.

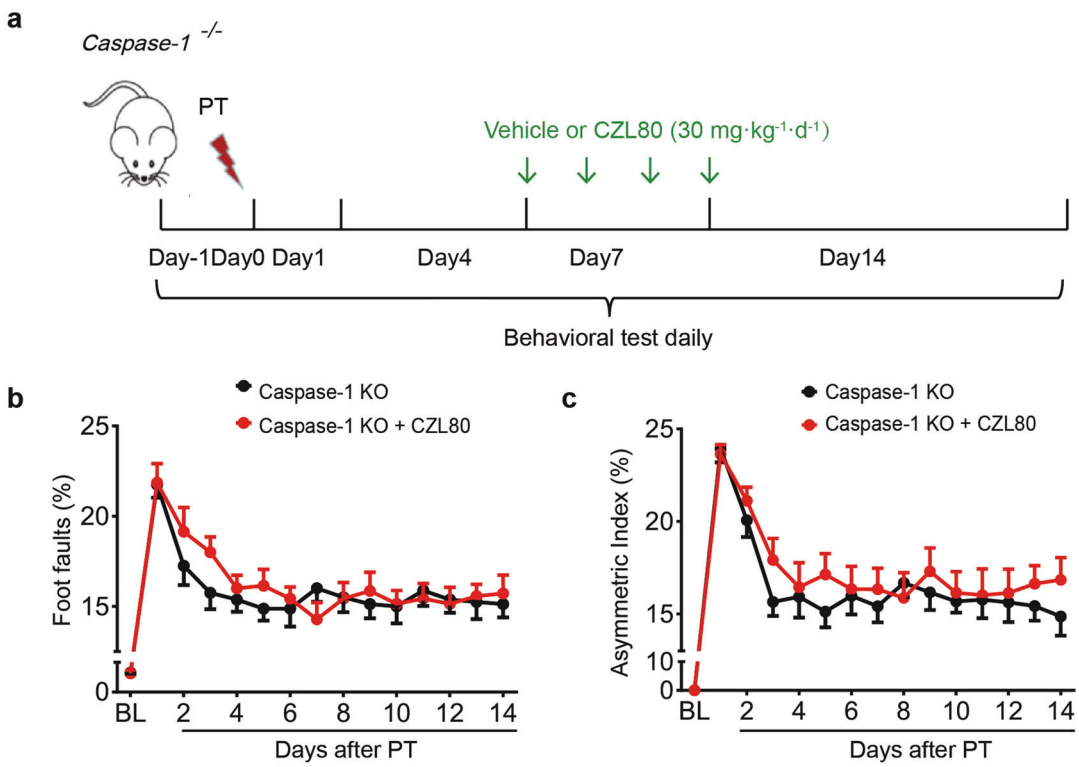

Fig. 4 *Caspase-1*$^{-/-}$ abolishes the therapeutic effect of CZL80. a Diagram showing the design of the experiments in this figure. CZL80 (30 mg·kg^{-1}·d^{-1}) or vehicle was intraperitoneally injected daily to *Caspase-1*$^{-/-}$ mice during Day4-7 and the neurological function was measured daily after photothrombotic stroke. **b** Foot fault of left forelimb in the grid-walking task and (**c**) Forelimb asymmetry in the cylinder task were determined. All results were represented as means ± SEM ($n = 8$ per group). Statistical significance was determined using one-way ANOVA with Tukey's post hoc test.

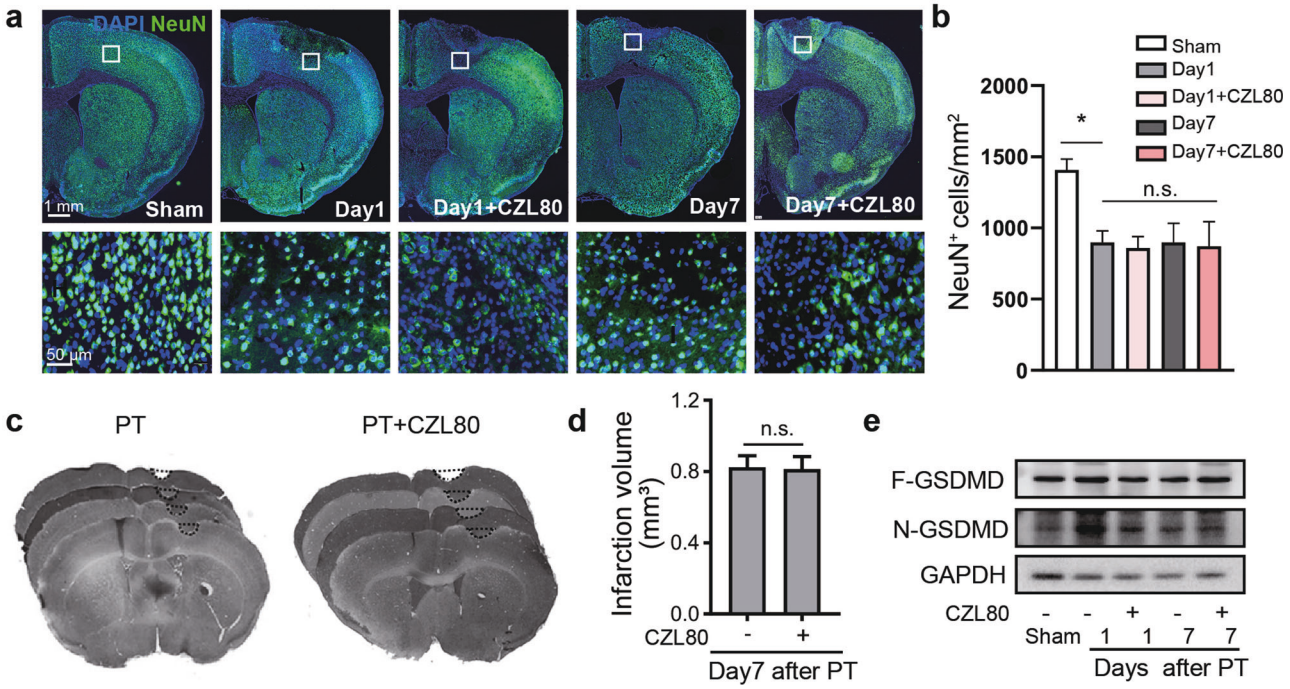

Fig. 5 CZL80 cannot inhibit neuronal death in PT-induced progressive stroke. a Mice were treated with CZL80 (30 mg·kg^{-1}·d^{-1}) for 1 or 7 days after the onset of photothrombosis. Representative images showing the staining of NeuN in indicated groups. The frames in upper panel were enlarged in lower panel. **b** Statistical data showing NeuN^{+} cells in the peri-infarct cortex of mice on Day1 and Day7 after ischemia and with CZL80 injection. ($n = 3$ animals per group). **c** Mice were treated with CZL80 (30 mg·kg^{-1}·d^{-1}) or vehicle daily for 7 days after PT onset, and the brain infarct was visualized by toluidine blue-stained sections on Day14. **d** Bar graph showed the volume of infarction from PT + vehicle and PT + CZL80 (30 mg/kg) mice. Results were represented as means ± SEM ($n = 3$ animals per group). Statistical significance was determined using one-way ANOVA with Tukey's post hoc test, n.s. (not significant vs. vehicle control). **e** Representative immunoblots showing full-length GSDMD (F-GSDMD) and cleaved GSDMD N-terminal (N-GSDMD) levels in the peri-infarct cortex from indicated groups. These experiments were repeated at least for 3 times independently.

after PT onset, suggesting the close association of microglia activation with PIS.

Given the Caspase-1 activation during progressive ischemic insult, we hypothesized CZL80 may attenuate microglial activation. We stained the microglia with Iba-1. To determine the effect of CZL80 on the activation of microglia, the expression of CD68 in microglia was measured by co-staining with microglial marker Iba-1. The results revealed that the co-localization of CD68 and Iba-1 after ischemia was suppressed by CZL80 treatment during 1–7 d or 4–7 d but not 1–4 d (Fig. 7a–c). To further verify the effect of CZL80 administration in different time periods on microglial activation, we determined the morphological changes of microglia. The increased soma area of microglia at Day7 was reduced by CZL80 administration during 1–7 d but not 4–7 d or 1–4 d (Fig. 7d). Consistent with the effect of CZL80 on neurological function, the circularity and solidity of microglia increased at Day7, which was inhibited by CZL80 administration during 1–7 d or 4–7 d but not 1–4 d (Fig. 7e, f). To confirm the effects of CZL80 on inhibiting microglia activation. CZL80 was incubated with primary cultured microglial cells treated with oxygen-glucose deprivation (OGD-R). It showed that CZL80 inhibited the upregulation of Caspase-1 by OGD-R (Fig. 7g, h). Overall, these results indicated microglial activation along with progressive neurological dysfunction, which can be inhibited by CZL80.

Angiogenesis has limited contribution to the pharmacological effects of CZL80 for progressive stroke

Improved angiogenesis enhances blood restore to ischemic brain tissue and ameliorates neurological dysfunction [36, 37]. Studies have reported that inhibition of Caspase-1 in endothelial cells can promote angiogenesis [38]. To further explore the effect of CZL80 on angiogenesis after cerebral ischemia in mice, we immunostained the Caspase-1 and endothelial marker CD31 at indicated time after PT insult. The results showed a fraction of Caspase-1 colocalized with endothelial cells (Fig. 8a). To the functional end, we measured the blood flow after PT [39], we found CZL80 only slightly improved the cerebral blood flow at Day4 but not Day7 after PT (Fig. 8b, c). Given that CZL80 showed its most prominent effect on Day7, these results implied that improved blood flow recovery at Day4 may not be involved in the protective effects of CZL80 in PT mice. Consistently, CZL80 did not further up-regulate the expression of vascular endothelial receptor 2 (VEGFR-2), a marker of angiogenesis, in PT mice at Day7 (Fig. 8d). Overall, these results suggest that angiogenesis and improved blood flow have limited contribution to the pharmacological effects of CZL80.

DISCUSSION

PIS is characterized by progressive aggravation of neurological dysfunction and poorer prognosis. Besides some defined causes, *e.g.*, secondary lacunar infarction, intracranial hemorrhage and cerebral edema, the mechanisms underlying PIS are far from being understood [2, 32, 40]. Previous studies implied the involvement of inflammasomal activation in PIS [13, 15, 41], however, the direct evidence has been missing [40]. Here we employed a photothrombotic stroke model, in which mice suffered a progressive neurological deficit during Day4-7 after ischemia, which reflected the characteristics of PIS [40] (Fig. 1c, d). In line with the neurological function changes, Caspase-1 showed a continuous upregulation during Day1-7, which was in line with

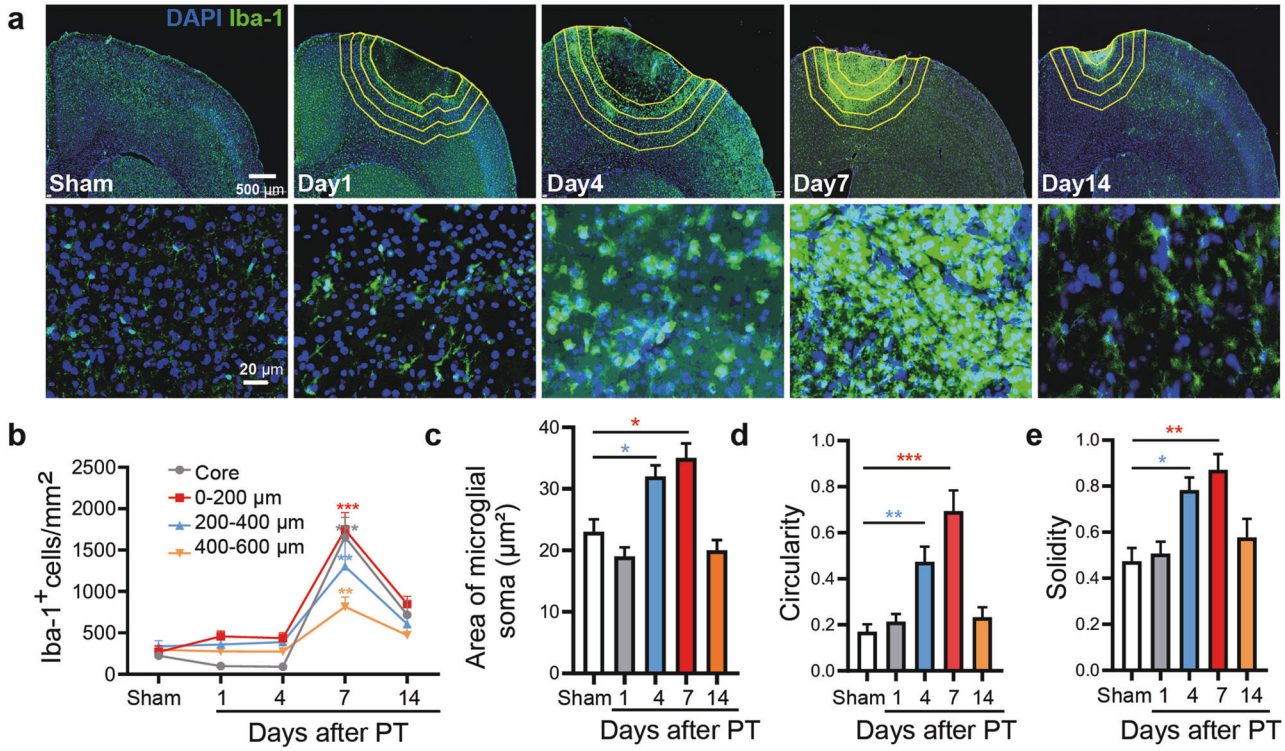

Fig. 6 Microglia activation in the progressive stroke. a Representative images showing the immunostaining of microglia (Iba-1) surrounding the infarct core at indicated time after photothrombosis (PT). The distance from ischemic core area is depicted by the yellow lines and the distance between the polylines is 200 μm. The lower representative images showing the morphology of microglia in the upper panels between 0 and 200 μm. **b** Quantification of microglia at different distances from the ischemic core on Day1, 4, 7, 14 after PT. **c**–**e** Quantitative analysis of the morphology of microglia. All results were represented as means ± SEM ($n = 3$ animals in each group). Statistical significance was determined using one-way ANOVA with Tukey's post hoc test, $^{*}P < 0.05$, $^{**}P < 0.01$ and $^{***}P < 0.001$ vs. Sham.

the progressive rather than acute neurological dysfunction. CZL80 reversed the neurological dysfunction at Day4-7 but showed minimum effect on Day1 after ischemia (Fig. 2). Moreover, *Caspase-1*$^{-/-}$ mice abolished the phenotypes of progressive, but not acute, neurological dysfunction (Fig. 4). All these data indicated a causative role of Caspase-1 in the progressive neurological function loss after ischemia. Previous studies emphasized a prompt neuronal injury by Caspase-1 activation in ischemic brains [23, 42, 43]. Together with the present study, we concluded that Caspase-1 may contribute discrepantly to the pathology of ischemic stroke. Particularly, the present study highlighted Caspase-1-related neuroinflammation plays a key role in the pathology of PIS.

The Caspase-1 inhibitors are limited by their poor bioavailability and safety concerns [16, 25]. To overcome these disadvantages, we previously designed the CZL80, a novel Caspase-1 inhibitor without significant toxicity and demonstrated its therapeutic effects against seizure and epilepsy [26, 27]. Here we found that CZL80 was competent to attenuate progressive, rather than acute neurological dysfunctions (Fig. 1). These data suggested the promising application of CZL80 in PIS. Remarkably, CZL80 administered as late as 4 days after ischemia was still effective, and its efficacy was equivalent to that of administration during Day1-7 (Supplementary Fig. S1). This wide therapeutic time-window of CZL80 is of potential value, because most of the drugs for stroke therapy are limited by their narrow therapeutic time-window [16, 21, 44]. As a comparison, the Caspase-1 inhibitors Ac-YVAD-CMK and VRT-018858 attenuated neurological dysfunction in the acute phase, but has no effect on the progressive impairment [44, 45]. Moreover, the time-window in which the neurological function deteriorated after primary insult seems to be crucial for long-term functional recovery [5, 33], and the benefits of CZL80 can last at least 43 days in our model (Fig. 3). This observation suggested that intervention of progressive neurological dysfunction after acute ischemia by CZL80 can be a promising strategy for PIS therapy.

Inflammasomes activation has been well-documented in various types of cells in ischemic brains [42, 43]. Neuronal Caspase-1 shows prompt activation and leads to neuronal pyroptosis by cleaving Gasdermins [19, 35, 46]. A variety of studies indicated that inhibiting the activation of microglia reduces acute ischemic brain injury [47–50]. However, CZL80 neither inhibited Gasdermin D cleavage, nor rescued neuronal death and acute neurological dysfunction (Fig. 5). Instead, we observed a delayed activation of microglial Caspase-1 during Day4-7, which was temporally consistent with the progressive functional damage (Fig. 6). These data suggested the delayed Caspase-1 activation in microglia was involved in the pathological process of progressive stroke. Additionally, the delayed activation of Caspase-1 may provide the rationale for the wide therapeutic time-window of CZL80. Activated microglia weaken the synaptic plasticity, which impede functional recovery of affected neurons [49]. This effect may not depend on the secretion of IL-1β, the most profound product of Caspase-1. In our PIS model, IL-1β did not alter along with that of Caspase-1 (Fig. 1e), also implied discrepant mechanisms for microglia to aggravate progressive neurological dysfunction. Intriguingly, it remains elusive why CZL80 did not reduce IL-1β as the other Caspase-1 inhibitors. Besides reasons due to the specificity of animal models, one possibility could be some enzymes other than Caspase-1 may cleave pro-IL-1β [51, 52]. Besides, we also confirmed that CZL80 failed to reinforce the expression of anti-inflammatory factors including IL-4 and IL-10 (data not shown). It seems that CZL80 did not confer its benefits by regulating the expression of

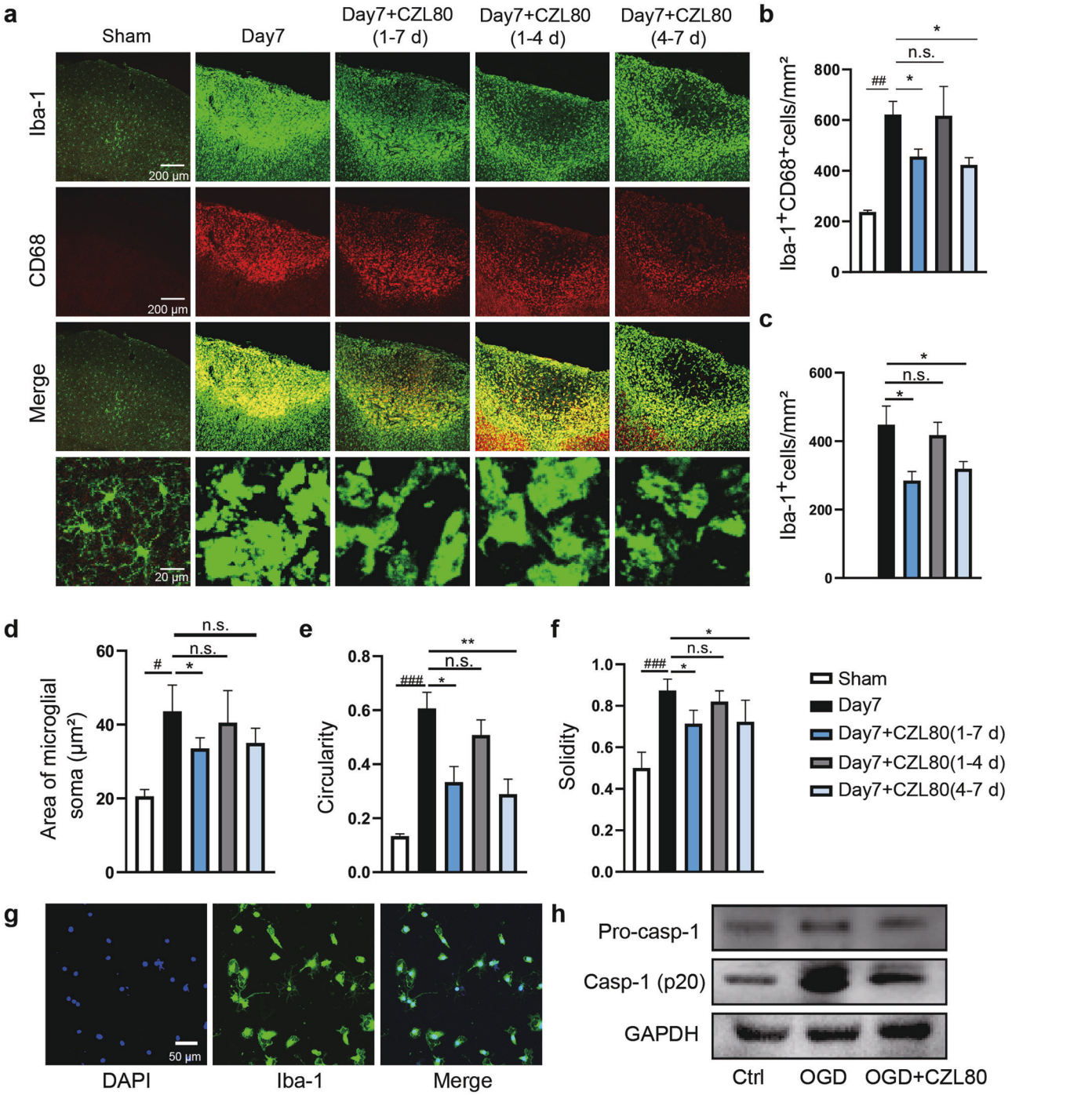

Fig. 7 CZL80 inhibits the activation of microglia. a Immunofluorescent staining of Iba-1-positive (green) and CD68-positive (red) microglia in and around the ischemic core area. Representative images (**a**) and quantitative analysis (**b**, **c**) showing the effect of CZL80 administration in different time periods on the immunostaining of Iba-1 and CD68 after PT. Statistical significance was determined using one-way ANOVA with Tukey's post hoc test, n.s. (not significant *vs*. Day7). $^{\#\#}P < 0.01$ vs. Sham, $^{*}P < 0.05$ vs. Day 7. **d**–**f** Quantitative analysis of the effects of CZL80 on soma area of microglia (**d**, $^{\#}P < 0.05$ vs. Sham, $^{*}P < 0.05$ vs. Day 7), circularity (**e**, $^{\#\#\#}P < 0.001$ vs. Sham, $^{*}P < 0.05$, $^{**}P < 0.01$ vs. Day 7) and solidity (**f**, $^{\#\#\#}P < 0.001$ vs. Sham, $^{*}P < 0.05$ vs. Day 7). **g** The primary cultured microglial cells were identified by staining with the microglia marker Iba-1. **h** CZL80 suppressed the expression of Caspase-1 in primary cultured microglia after OGD/R, as measured by western blot. All of the data are shown as mean ± SEM. These experiments were repeated at least for 3 times independently.

inflammatory factors. Indeed, Caspase-1 has a wide spectrum of substrates besides inflammatory factors, which endows Caspase-1 the ability to regulate a variety of cellular functions, including metabolism, proliferation, and proteasomal degradation etc. [53, 54]. It is presumably that different Caspase-1 inhibitors, including CZL80, may have preference on distinct substrate cleavage by Caspase-1. Further studies are needed to address the pharmacological features of CZL80.

Taken together, the present study indicated that the microglial Caspase-1 activation was closely involved in the neurological dysfunction in PIS. Inhibition of the delayed Caspase-1 activation in microglia may provide a critical strategy for PIS therapy.

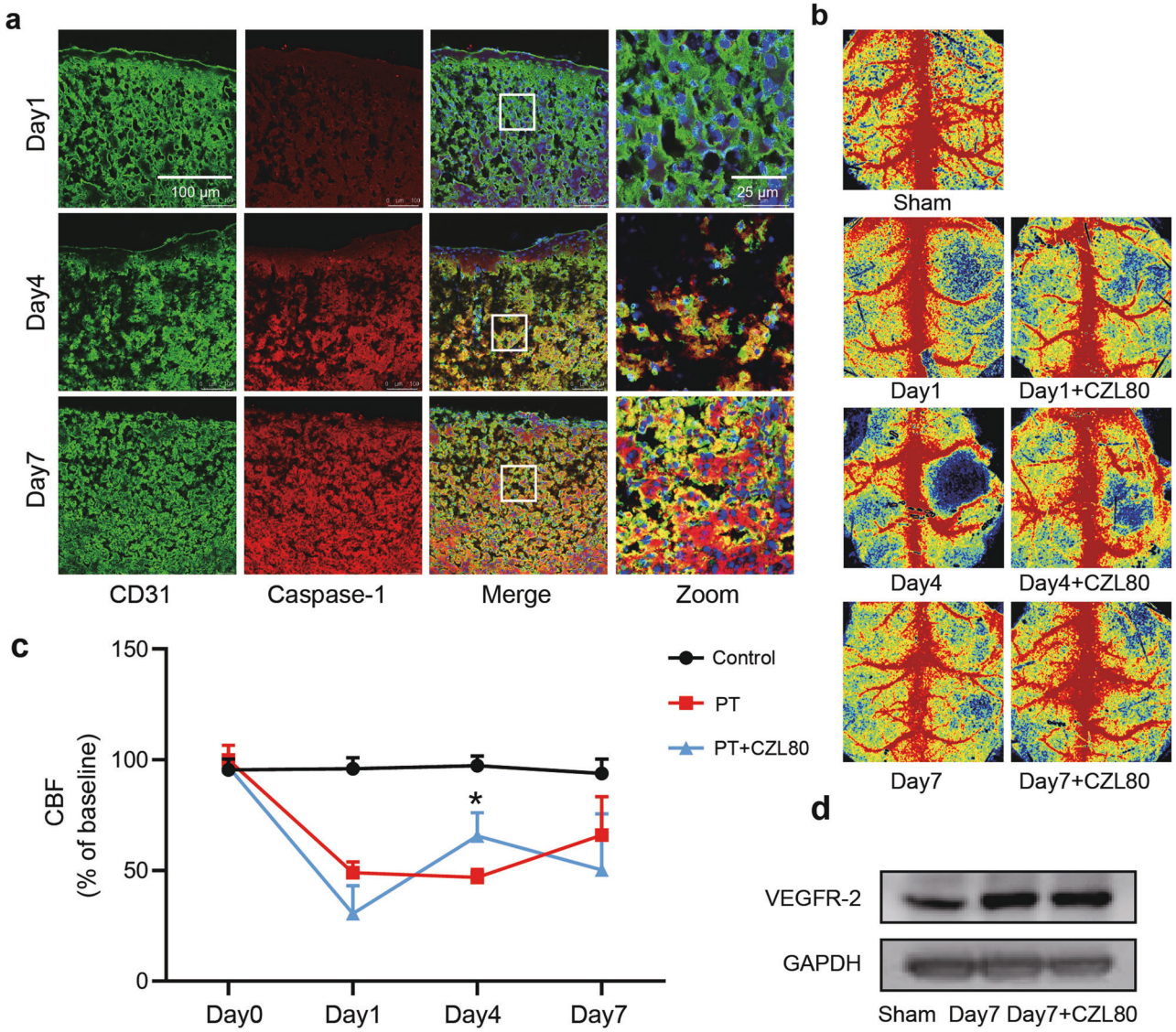

Fig. 8 Angiogenesis and improved blood flow have limited contribution to the pharmacological effects of CZL80. a Representative images showing the immunofluorescent staining of Caspase-1 with endothelial cells on Day1, 4, 7 after photothrombosis. CD31 was taken as markers of endothelial cells (CD31). **b** Representative cerebral blood flow images from indicated groups. **c** Statistical data showing changes in CBF for the Sham group, PT group and PT + CZL80 group on Day0, Day1, Day4 and Day7. Results were represented as means ± SEM ($n = 5–6$ animals per group). Statistical significance was determined using one-way ANOVA with Tukey's post hoc test, $^*P < 0.05$ vs. PT group. **d** Representative immunoblots showing VEGFR-2 in the peri-infarct cortex from indicated groups. These experiments were repeated at least for 3 times independently.

Moreover, we identified the therapeutic effect of CZL80, a new Caspase-1 inhibitor, on rescuing the progressive neurological deficit with a wide time-window. CZL80 can be a promising drug for PIS therapy.

ACKNOWLEDGEMENTS

This work was funded by the National Natural Science Foundation of China (82173792 and 81822044), Zhejiang Provincial Natural Science Foundation (LZ21H310001) and the Starry Night Science Fund of Zhejiang University Shanghai Institute for Advanced Study (SN-ZJU-SIAS-0011). We are grateful to the Imaging Facilities, Zhejiang University School of Medicine for the help in microscopy.

AUTHOR CONTRIBUTIONS

XNZ and ZC designed research. LP and WDT planned and performed the experiments, analyzed the data and edited the paper. KW, QFF, MRL and ZXW participated in the biochemistry experiments. YW, SLC, GH, TJH and WWH participated in the project discussion and analyzed the data. LP contributed to writing the paper, and XNZ reviewed/edited the paper.

ADDITIONAL INFORMATION

Supplementary information The online version contains supplementary material available at https://doi.org/10.1038/s41401-022-00913-7.

Competing interests: The authors declare no competing interests.

REFERENCES

1. Mendis S, Davis S, Norrving B. Organizational update: the world health organization global status report on noncommunicable diseases 2014; one more landmark step in the combat against stroke and vascular disease. Stroke. 2015;46:e121–2.
2. Birschel P, Ellul J, Barer D. Progressing stroke: towards an internationally agreed definition. Cerebrovasc Dis. 2004;17:242–52.

3. Siegler JE, Boehme AK, Albright KC, George AJ, Monlezun DJ, Beasley TM, et al. A proposal for the classification of etiologies of neurologic deterioration after acute ischemic stroke. J Stroke Cerebrovasc Dis. 2013;22:e549–56.
4. Caplan LR. Worsening in ischemic stroke patients: is it time for a new strategy? Stroke. 2002;33:1443–5.
5. Lin YH, Dong J, Tang Y, Ni HY, Zhang Y, Su P, et al. Opening a new time window for treatment of stroke by targeting HDAC2. J Neurosci. 2017;37:6712–28.
6. Anrather J, Iadecola C. Inflammation and stroke: an overview. Neurotherapeutics. 2016;13:661–70.
7. Chamorro Á, Dirnagl U, Urra X, Planas AM. Neuroprotection in acute stroke: targeting excitotoxicity, oxidative and nitrosative stress, and inflammation. Lancet Neurol. 2016;15:869–81.
8. Lambertsen KL, Finsen B, Clausen BH. Post-stroke inflammation-target or tool for therapy? Acta Neuropathol. 2019;137:693–714.
9. An C, Shi Y, Li P, Hu X, Gan Y, Stetler RA, et al. Molecular dialogs between the ischemic brain and the peripheral immune system: dualistic roles in injury and repair. Prog Neurobiol. 2014;115:6–24.
10. Wang R, Pu H, Ye Q, Jiang M, Chen J, Zhao J, et al. Transforming growth factor beta-activated kinase 1-dependent microglial and macrophage responses aggravate long-term outcomes after ischemic stroke. Stroke. 2020;51:975–85.
11. Vila N, Castillo J, Dávalos A, Chamorro A. Proinflammatory cytokines and early neurological worsening in ischemic stroke. Stroke. 2000;31:2325–9.
12. Yang C, Hawkins KE, Dore S, Candelario-Jalil E. Neuroinflammatory mechanisms of blood-brain barrier damage in ischemic stroke. Am J Physiol Cell Physiol. 2019;316:C135–C53.
13. Yesin M, Cagdas M, Karabag Y, Rencuzogullari I, Burak C, Kalcik M, et al. Assessment of the relationship between C-reactive protein-to-albumin ratio and slow coronary flow in patients with stable angina pectoris. Coron Artery Dis. 2019;30:505–10.
14. Schroder K, Tschopp J. The inflammasomes. Cell. 2010;140:821–32.
15. Sanjo N, Nose Y, Shishido-Hara Y, Mizutani S, Sekijima Y, Aizawa H, et al. A controlled inflammation and a regulatory immune system are associated with more favorable prognosis of progressive multifocal leukoencephalopathy. J Neurol. 2019;266:369–77.
16. Yang S, Wang H, Yang Y, Wang R, Wang Y, Wu C, et al. Baicalein administered in the subacute phase ameliorates ischemia-reperfusion-induced brain injury by reducing neuroinflammation and neuronal damage. Biomed Pharmacother. 2019;117:109102.
17. Boucher D, Monteleone M, Coll RC, Chen KW, Ross CM, Teo JL, et al. Caspase-1 self-cleavage is an intrinsic mechanism to terminate inflammasome activity. J Exp Med. 2018;215:827–40.
18. Elliott EI, Sutterwala FS. Initiation and perpetuation of NLRP3 inflammasome activation and assembly. Immunol Rev. 2015;265:35–52.
19. Li J, Hao JH, Yao D, Li R, Li XF, Yu ZY, et al. Caspase-1 inhibition prevents neuronal death by targeting the canonical inflammasome pathway of pyroptosis in a murine model of cerebral ischemia. CNS Neurosci Ther. 2020;26:925–39.
20. Rashad S, Niizuma K, Sato-Maeda M, Fujimura M, Mansour A, Endo H, et al. Early BBB breakdown and subacute inflammasome activation and pyroptosis as a result of cerebral venous thrombosis. Brain Res. 2018;1699:54–68.
21. Li Q, Dai Z, Cao Y, Wang L. Caspase-1 inhibition mediates neuroprotection in experimental stroke by polarizing M2 microglia/macrophage and suppressing NF-kappaB activation. Biochem Biophys Res Commun. 2019;513:479–85.
22. Huang FP, Wang ZQ, Wu DC, Schielke GP, Sun Y, Yang GY. Early NF-kappaB activation is inhibited during focal cerebral ischemia in interleukin-1beta-converting enzyme deficient mice. J Neurosci Res. 2003;73:698–707.
23. Schielke GP, Yang GY, Shivers BD, Betz AL. Reduced ischemic brain injury in interleukin-1 beta converting enzyme-deficient mice. J Cereb Blood Flow Metab. 1998;18:180–5.
24. Aglietti RA, Dueber EC. Recent insights into the molecular mechanisms underlying pyroptosis and Gasdermin family functions. Trends Immunol. 2017;38:261–71.
25. Fischer U, Schulze-Osthoff K. Apoptosis-based therapies and drug targets. Cell Death Differ. 2005;12:942–61. Suppl 1.
26. Tang Y, Feng B, Wang Y, Sun H, You Y, Yu J, et al. Structure-based discovery of CZL80, a caspase-1 inhibitor with therapeutic potential for febrile seizures and later enhanced epileptogenic susceptibility. Br J Pharmacol. 2020;177:3519–34.
27. Xu C, Zhang S, Gong Y, Nao J, Shen Y, Tan B, et al. Subicular Caspase-1 contributes to pharmacoresistance in temporal lobe epilepsy. Ann Neurol. 2021;90:377–90.
28. Clarkson AN, Huang BS, Macisaac SE, Mody I, Carmichael ST. Reducing excessive GABA-mediated tonic inhibition promotes functional recovery after stroke. Nature. 2010;468:305–9.
29. Wu XL, Lu SS, Liu MR, Tang WD, Chen JZ, Zheng YR, et al. Melatonin receptor agonist ramelteon attenuates mouse acute and chronic ischemic brain injury. Acta Pharmacol Sin. 2020;41:1016–24.
30. Shen Z, Zheng Y, Wu J, Chen Y, Wu X, Zhou Y, et al. PARK2-dependent mitophagy induced by acidic postconditioning protects against focal cerebral ischemia and extends the reperfusion window. Autophagy. 2017;13:473–85.
31. Clarkson AN, Overman JJ, Zhong S, Mueller R, Lynch G, Carmichael ST. AMPA receptor-induced local brain-derived neurotrophic factor signaling mediates motor recovery after stroke. J Neurosci. 2011;31:3766–75.
32. Weimar C, Mieck T, Buchthal J, Ehrenfeld CE, Schmid E, Diener HC. German Stroke Study Collaboration. Neurologic worsening during the acute phase of ischemic stroke. Arch Neurol. 2005;62:393–7.
33. Tang Y, Lin YH, Ni HY, Dong J, Yuan HJ, Zhang Y, et al. Inhibiting Histone Deacetylase 2 (HDAC2) promotes functional recovery from stroke. J Am Heart Assoc. 2017;6:e007236.
34. Zhang WH, Wang X, Narayanan M, Zhang Y, Huo C, Reed JC, et al. Fundamental role of the Rip2/caspase-1 pathway in hypoxia and ischemia-induced neuronal cell death. Proc Natl Acad Sci USA. 2003;100:16012–7.
35. Zhang D, Qian J, Zhang P, Li H, Shen H, Li X, et al. Gasdermin D serves as a key executioner of pyroptosis in experimental cerebral ischemia and reperfusion model both in vivo and in vitro. J Neurosci Res. 2019;97:645–60.
36. Beck H, Plate KH. Angiogenesis after cerebral ischemia. Acta Neuropathol. 2009;117:481–96.
37. Zhang X, Chen XP, Lin JB, Xiong Y, Liao WJ, Wan Q. Effect of enriched environment on angiogenesis and neurological functions in rats with focal cerebral ischemia. Brain Res. 2017;1655:176–85.
38. Lopez-Pastrana J, Ferrer LM, Li YF, Xiong X, Xi H, Cueto R, et al. Inhibition of Caspase-1 activation in endothelial cells improves angiogenesis: a novel therapeutic potential for ischemia. J Biol Chem. 2015;290:17485–94.
39. Qiu ZD, Deng G, Yang J, Min Z, Li DY, Fang Y, et al. A new method for evaluating regional cerebral blood flow changes: laser speckle contrast imaging in a C57BL/6J mouse model of photothrombotic ischemia. J Huazhong Univ Sci Technol Med Sci. 2016;36:174–80.
40. Seners P, Baron JC. Revisiting 'progressive stroke': incidence, predictors, pathophysiology, and management of unexplained early neurological deterioration following acute ischemic stroke. J Neurol. 2018;265:216–25.
41. Comarmond C, Biard L, Lambert M, Mekinian A, Ferfar Y, Kahn JE, et al. Long-term outcomes and prognostic factors of complications in takayasu arteritis: a multicenter study of 318 patients. Circulation. 2017;136:1114–22.
42. Abulafia DP, de Rivero Vaccari JP, Lozano JD, Lotocki G, Keane RW, Dietrich WD. Inhibition of the inflammasome complex reduces the inflammatory response after thromboembolic stroke in mice. J Cereb Blood Flow Metab. 2009;29:534–44.
43. Strowig T, Henao-Mejia J, Elinav E, Flavell R. Inflammasomes in health and disease. Nature. 2012;481:278–86.
44. Fann DY, Lee SY, Manzanero S, Tang SC, Gelderblom M, Chunduri P, et al. Intravenous immunoglobulin suppresses NLRP1 and NLRP3 inflammasome-mediated neuronal death in ischemic stroke. Cell Death Dis. 2013;4:e790.
45. Ross J, Brough D, Gibson RM, Loddick SA, Rothwell NJ. A selective, non-peptide caspase-1 inhibitor, VRT-018858, markedly reduces brain damage induced by transient ischemia in the rat. Neuropharmacology. 2007;53:638–42.
46. Liu X, Zhang Z, Ruan J, Pan Y, Magupalli VG, Wu H, et al. Inflammasome-activated gasdermin D causes pyroptosis by forming membrane pores. Nature. 2016;535:153–8.
47. Chen AQ, Fang Z, Chen XL, Yang S, Zhou YF, Mao L, et al. Microglia-derived TNF-alpha mediates endothelial necroptosis aggravating blood brain-barrier disruption after ischemic stroke. Cell Death Dis. 2019;10:487.
48. Ma J, Zhang J, Hou WW, Wu XH, Liao RJ, Chen Y, et al. Early treatment of minocycline alleviates white matter and cognitive impairments after chronic cerebral hypoperfusion. Sci Rep. 2015;5:12079.
49. Ma Y, Wang J, Wang Y, Yang GY. The biphasic function of microglia in ischemic stroke. Prog Neurobiol. 2017;157:247–72.
50. Xiong XY, Liu L, Yang QW. Functions and mechanisms of microglia/macrophages in neuroinflammation and neurogenesis after stroke. Prog Neurobiol. 2016;142:23–44.
51. Kavita U, Mizel SB. Differential sensitivity of interleukin-1 alpha and -beta precursor proteins to cleavage by calpain, a calcium-dependent protease. J Biol Chem. 1995;270:27758–65.
52. Kayagaki N, Warming S, Lamkanfi M, Vande Walle L, Louie S, Dong J, et al. Non-canonical inflammasome activation targets caspase-11. Nature. 2011;479:117–21.
53. Denes A, Lopez-Castejon G, Brough D. Caspase-1: is IL-1 just the tip of the ICEberg? Cell Death Dis. 2012;3:e338.
54. Keller M, Ruegg A, Werner S, Beer HD. Active caspase-1 is a regulator of unconventional protein secretion. Cell. 2008;132:818–31.